

**Fermi National Accelerator Laboratory**

**TM-1534**

**Comparison of Muon Flux Measurements  
to Halo Monte Carlo Predictions**

Linda G. Stutte  
Fermi National Accelerator Laboratory  
P.O. Box 500, Batavia, Illinois

July 18, 1988



Operated by Universities Research Association Inc. under contract with the United States Department of Energy

TM-1534  
Linda G. Stutte  
July 18, 1988

## COMPARISON OF MUON FLUX MEASUREMENTS TO HALO MONTE CARLO PREDICTIONS

### I. Introduction

Experiment E-782 has been approved to run during the next fixed target cycle in a fast-spill muon beam aimed at the Tohoku bubble chamber, located in Lab F. New construction is necessary to provide this beam. Initial feasibility tests were carried out during the last fixed target run, measuring both muon fluxes and background halo rates, as a function of several parameters. These test results are compared in detail with the predictions of the Monte Carlo program HALO<sup>1</sup>, and can be used as a benchmark for design of the final beamline.

### II. Description of beamline and counter setup

The beamline used to carry out the test measurements was the NH beamline (shown in Figure 1), normally used to provide a calibration beam to the Lab C neutrino detector (located further downstream from Lab F). Briefly, this beamline is a low acceptance, small momentum bite transport system, with momentum selection available up to approximately 400 GeV. The central production angle can be varied over several milliradians (depending on the momentum selected), including zero-degree production. The target selected for these measurements was a one interaction length Aluminum target. The non-interacting primary protons are dumped in enclosure NE8, with a back-up dump located within the pipe between enclosures NE8-9. Momentum selection is determined by the setting of the NE9 dipole string (NH9W), with the NEB dipoles (NHBW1) set to maximize

transmission. A point-to-point focus is made from the target to the momentum defining collimator (NHACH) located in enclosure NEA, at which point there is also a field lens. The rest of the optics forms a point-to-parallel focus towards the detectors. Intensity can be controlled with two collimators (NH9CH and NH9CV) located in enclosure NE9. A moveable dump module is situated in the upstream end of Lab F, which serves as an absorber for muon beam transport to Lab C. This dump was placed in the beam for all of the muon measurements described here.

The beamline was first tuned to 150 GeV, transporting negative pions and kaons all the way to Lab F. The targetting angle magnet (NH8UE) was adjusted to select zero-degree production, in order to maximize rates. All collimators were kept fully open. Initially, 15 feet of 8-inch diameter polyethelene slugs were inserted into the upstream end of enclosure NEB, to provide an absorber. Then the NHBW1 dipoles were adjusted to maximize rates. The current settings for all beamline magnets were then scaled from the 150 GeV tuned values to those used at the other energies: 50, 100, 200, 250 and 300 GeV.

Most of the data were taken with an absorber located in the downstream end of enclosure NE9. This absorber consisted of 6 feet of 5-inch square beryllium and 28.67 feet of 8-inch diameter polyethelene slugs. For an absorber position study, these data were combined with the NEB poly data, and two other points obtained by closing the collimators NH9CH and NHACH, respectively.

Figure 2 shows the scintillation counters used in Lab F. At the front of Lab F, a 4-inch square counter was used to define the beam trajectory. Following the dump, two 24-inch square counters were placed on moveable stands. These counters could be lined up in order to measure coincidences over a 24-inch square area, or moved apart to be used in coincidence with the 10-inch square paddle, as it was stepped both vertically and horizontally in order to measure the beam profile. In addition, a 4-inch wide by 1.5-inch high coincidence was set up in the downstream end of NEB. This was added in coincidence with the Lab F counters, in order to get a measure of muons in the beam. The Lab F counters alone then contain the sum of these muons plus additional halo muons which left the beamline transport system at some upstream location. Since not all data sets included the coincidences involving the NEB counters, for uniformity no subtractions will be made to present the halo rates alone, except as noted.

In summary, as a measure of beam muon rates, coincidences were available over a 4-inch square, a 10-inch square and a 24-inch square. For beam plus muon halo rates, coincidences were available over a 10-inch square and a 24-inch square.

Finally, it must be noted that the Lab F counters picked up considerable spray from the adjacent NEAST beamline, which was running at a much higher intensity than the NH line. For each data set, an NH beamline off point was taken, in order to subtract out the effect of this background.

### III. Description of HALO Monte Carlo set-up

To simulate the NH beamline, the Monte Carlo program HALO was used with a production model formula<sup>2</sup> based on data taken at CERN with 400 GeV protons incident on beryllium. A slight modification was made to the program in order to model the actual vertical position of the targetted proton beam, which was 6.5 mm higher than beamline center. In order to simulate the beam dump which followed the target, it was divided into four sections, each of which had a one inch square opening, and was vertically offset from the next by successive 0.075-inch steps. Flags of the appropriate area were placed along the beamline at the scintillator locations and histograms were made of beam and halo particles with conditions imposed to match the actual logical coincidences which had been set up. Separate pi- and K- runs were made, and the numbers combined with appropriate weights. It was found that the minimum momentum cut-off for generated parents needed to be no more than 1/2 the central momentum, in order to avoid underestimating halo rates. Two distinct sets of runs were made, one using magnetic fields determined from the actual as-run currents, and one with ideal magnetic fields determined from TRANSPORT<sup>3</sup> calculations. Unless otherwise noted, the set using as-run currents will be compared to the data.

### IV. Comparison of Z-distributions

Figure 3 shows 200 GeV muon rates per  $10^{11}$  protons on target as a

function of absorber position from the production target. The left two plots are the Monte Carlo predictions, the right two plots are the actual data. The top two plots show coincidences of Lab F counters of various sizes with the NEB counters ("BEAM"), and the bottom two plots show Lab F counters alone ("BEAM+HALO"). In this and subsequent figures, error bars for both data and Monte Carlo are statistical only. The 10- and 24-inch BEAM coincidences were not available for the deepest absorber position. For the first three positions, data and Monte Carlo agree to better than 20%, for the most part data being slightly higher than predictions. For the deepest absorber position, the data continue to rise essentially linearly with absorber position, while the Monte Carlo shows a turn-over in rates.

Figure 4 shows the dependence of HALO/BEAM as a function of absorber position for 200 GeV data. In this figure, the 24-inch BEAM data was subtracted from the 24-inch BEAM+HALO data, in order to directly present halo rates. The figure clearly shows the advantage of locating the absorber as close as possible to the end of the transport system, in order to maximize signal to noise.

## V. Comparison of Energy distributions

Figure 5 compares muon rates per  $10^{11}$  protons on target as a function of energy for the Beryllium and polyethelene absorber located at the downstream end of enclosure NE9. As in Figure 3, the left two plots are the Monte Carlo predictions, the right two plots are data. The top two plots are BEAM, and the bottom two plots are BEAM+HALO, for various size counters. The major difference to be noted here is that the Monte Carlo predicts a harder momentum spectrum for BEAM muons than actually observed. The BEAM+HALO rates (dominated by halo particles) agree much better.

Figure 6 shows the dependence of HALO/BEAM as a function of energy for the Be/poly data. As in Figure 4, the 24-inch BEAM data was subtracted from the 24-inch BEAM+HALO data, in order to directly present halo rates. The HALO/BEAM rate is seen to increase exponentially with increasing beam energy.

Figure 7 shows muon rate measurements as a function of beam energy for the most upstream absorber position (left plots) and for the

most downstream absorber position (right plots). Apart from the large difference in rates between the two data sets, the most striking feature of this figure is the absence of a turn-over at higher momentum in the BEAM+HALO rates for the upstream data set.

## VI. Comparison of beam size

In order to get a measure of the muon beam size in Lab F, the two 24-inch scintillation counters were placed side by side, to cover the widest possible area. The 10-inch counter was mounted on a moveable stand, and was first swept horizontally across the beam at beamline elevation in 2.5-inch steps, and then swept vertically across the beam on horizontal beamline center, also in 2.5-inch steps. Data were then available for BEAM and BEAM+HALO profiles to be compared to Monte Carlo predictions. These scans were done several times. An early data set did not have the BEAM coincidences set up. This data set however was taken at a much higher intensity on target than a later data set, for which the BEAM coincidences existed. In addition, the earlier data set was taken when the NEAST beamline happened to be off, thus reducing complications from a large background subtraction. For these two reasons, the early BEAM+HALO data set will be compared to Monte Carlo predictions, along with the later BEAM data. Figure 8 shows the early and later BEAM+HALO data sets, with the lines connecting the points from the early data set. These data were taken at 200 GeV, with the Be/poly absorber. The figure illustrates that the NEAST background subtraction (made to all data presented in this paper) is being done correctly.

Figure 9 compares the beam sizes for data and Monte Carlo predictions. The lines connect the points of the Monte Carlo predictions. The top plot is a horizontal scan, the bottom plot is a vertical scan. In each plot, both the BEAM and BEAM+HALO profiles are shown. The BEAM profiles compare well with predictions, but the BEAM+HALO data exhibit a much stronger focus than the Monte Carlo would predict.

In Figure 10, these same 200 GeV data profiles are compared to Monte Carlo predictions using ideal currents, as determined by TRANSPORT. Again, the lines connect the points of the Monte Carlo predictions. Here, the shapes of the distributions agree much better, but the absolute rates disagree, especially for the BEAM profiles. Probably an

average of as-run and ideal Monte Carlo predictions would fit the data best.

Finally, Figure 11 shows the BEAM profiles obtained at two different energies, 200 and 150 GeV. The lines connect the points of the 200 GeV data set. No difference in size was observed.

## VII. Comparison of momentum spectra

In order to maximize beam rates, the magnet NHBW1 was adjusted. This current scan provides an indirect way to estimate the momentum bite of the muon beam. If the Monte Carlo is run several times, always changing the value of the magnetic field in NHBW1, and the results of this scan agree well with the data, then the muon momentum spectra are probably close to that of the Monte Carlo predictions.

Figure 12 shows a 200 GeV NHBW1 scan, using the Be/poly absorber. The top plot shows the 4-inch BEAM coincidence rate, along with another coincidence that demanded the beam travel through the entire length of Lab F. The middle plot shows the 10- and 24-inch BEAM rates, and the bottom plot shows the 10- and 24-inch BEAM+HALO rates. In the top plot, a dip in both rates is evident at 2050 amps. As one integrates over larger and larger cross sections, the scans get broader as a function of current, indicating larger momentum spectra.

Figure 13 shows the Monte Carlo predictions for the same BEAM and BEAM+HALO rates. The 4-inch BEAM and the 10- and 24-inch BEAM+HALO rates agree quite well with the data of Figure 12. The agreement of the 10-inch BEAM rates is less good, and the 24-inch Monte Carlo prediction is approximately 20% narrower than the data.

The Monte Carlo momentum spectra for these different coincidences are shown in Figure 14. The 4-inch BEAM peak full width half maximum (FWHM) momentum bite is 7.3%. The 10- and 24-inch BEAM peak FWHM momentum bites are 9.7%. The 10- and 24-inch BEAM+HALO peak FWHM momentum bites are 10.8% and 12.0%, respectively. In the BEAM+HALO spectra, the low momentum halo tail is quite evident.

If one repeats these Monte Carlo scans with ideal magnet currents,

one gets sharper BEAM distributions (Figure 15). The momentum spectra for the ideal case are also somewhat tighter (about 6% for the BEAM coincidences, and 7% for the BEAM+HALO coincidences), shown in Figure 16.

## VIII. Conclusions

In this detailed study of muon production rates comparing data to predictions of the Monte Carlo program HALO, excellent agreement (within about 20%) has been observed over a variety of variables: absorber location, beamline energy, beam size and momentum bite.

## IX. Acknowledgements

This study could not have been possible without the generous assistance of Gordon Koizumi during data taking, and the invaluable help provided by Anthony Malensek and Jorge Morfin in setting up the HALO decks.

## References:

1. Ch. Iselin, "HALO, a Computer Program to Calculate Muon Production", CERN Report 74-17, 1974.
2. A. J. Malensek, "Emperical Formula for Thick Target Production", Fermilab note FN-341, 1981.
3. K. L. Brown, et al, "TRANSPORT, a Computer Program for Designing Charged Particle Beam Transport Systems", SLAC-91, 1977.

## Figure Captions:

1. NH beamline layout.
2. Lab F scintillation counter layout.
3. Muon rates per  $10^{11}$  protons on target as a function of absorber position from the production target, Monte Carlo (left plots) and data (right plots): BEAM coincidences (top plots) and BEAM+HALO coincidences (bottom plots), using various size Lab F scintillation counters. Lines shown just connect the points. For the data, the BEAM coincidences for 24" and 10" Lab F counters were not available.
4. HALO in the 24" Lab F counter divided by BEAM in the 4" Lab F counter as a function of absorber position from the production target.
5. Muon rates per  $10^{11}$  protons on target as a function of energy, Monte Carlo (left plots) and data (right plots): BEAM coincidences (top plots) and BEAM+HALO coincidences (bottom plots), using various size Lab F scintillation counters. These scans were done for the Beryllium + polyethelene absorber located in downstream NE9.
6. HALO in the 24" Lab F counter divided by BEAM in the 4" Lab F counter as a function of energy, for the Be/poly absorber located in downstream NE9.
7. Muon rates per  $10^{11}$  protons on target as a function of energy, data taken at the most upstream absorber location (left plots) and data taken at the most downstream absorber location (right plots): BEAM coincidences (top plots) and BEAM+HALO coincidences (bottom plots), using various size Lab F scintillation counters.
8. Muon rates per  $10^{11}$  protons on target during BEAM+HALO size scans, HORIZONTAL (top plot) and VERTICAL (bottom plot), for two different data sets: a high intensity scan with little NEAST beamline background (open squares), and a low intensity scan with the NEAST beamline on (filled diamonds). The lines connect the high intensity data points. These data were taken at 200 GeV, with the Be/poly absorber.

9. Muon rates per  $10^{11}$  protons on target during beam size scans, HORIZONTAL (top plot) and VERTICAL (bottom plot) compared to Monte Carlo predictions. Each plot contains both the BEAM (squares) and the BEAM+HALO (triangles) ratios. The data are shown using the filled points, and the Monte Carlo predictions are shown using the open points, with lines connecting them. The plots are for 200 GeV, using the Be/poly absorber.
10. Beam size scans, as in Figure 9, but here using the ideal magnet settings, as determined by TRANSPORT.
11. Beam size scans, as in Figure 9, but here comparing data taken at 150 GeV with that obtained at 200 GeV, both sets using the Be/poly absorber.
12. Muon rates per  $10^{11}$  protons on target as a function of current in the large dipole string NHBW1, located in the enclosure upstream of Lab F, for various size Lab F scintillation counters: BEAM coincidences (top and middle plots), and BEAM+HALO coincidences (bottom plot). These data were taken at 200 GeV, with the Be/poly absorber.
13. Muon rates per  $10^{11}$  protons on target as a function of current in the NHBW1 magnet string, for various size Lab F scintillation counters as predicted by the Monte Carlo program. BEAM coincidences (top and middle plots), and BEAM+HALO coincidences (bottom plot).
14. Momentum spectra as predicted by the Monte Carlo program for BEAM and BEAM+HALO coincidences given in Figure 13.
15. Muon rates per  $10^{11}$  protons on target as a function of current in the NHBW1 magnet string, as in Figure 13, as predicted by the Monte Carlo program using the ideal magnet settings from TRANSPORT.
16. Momentum spectra as in Figure 14, but for the ideal magnet settings.

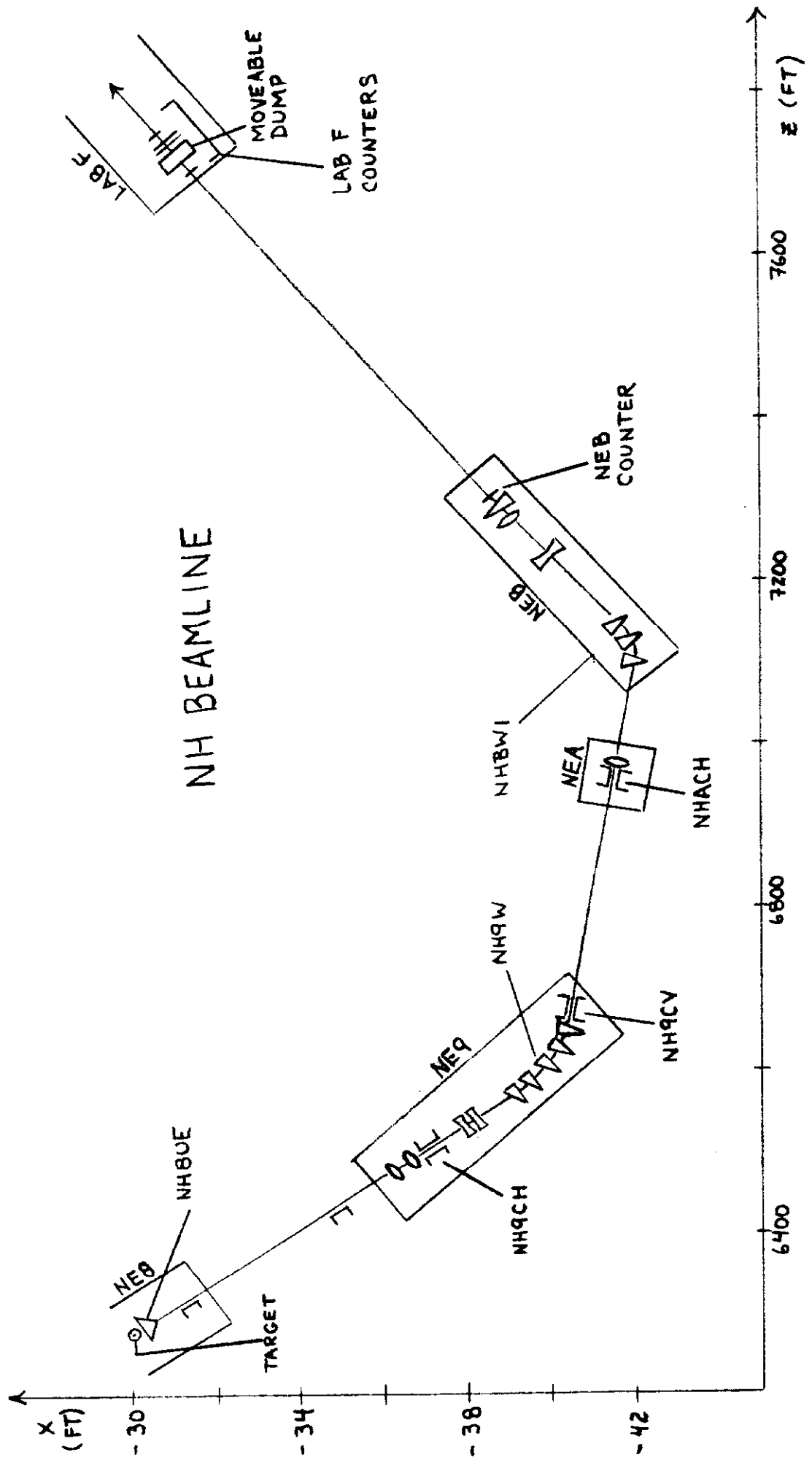
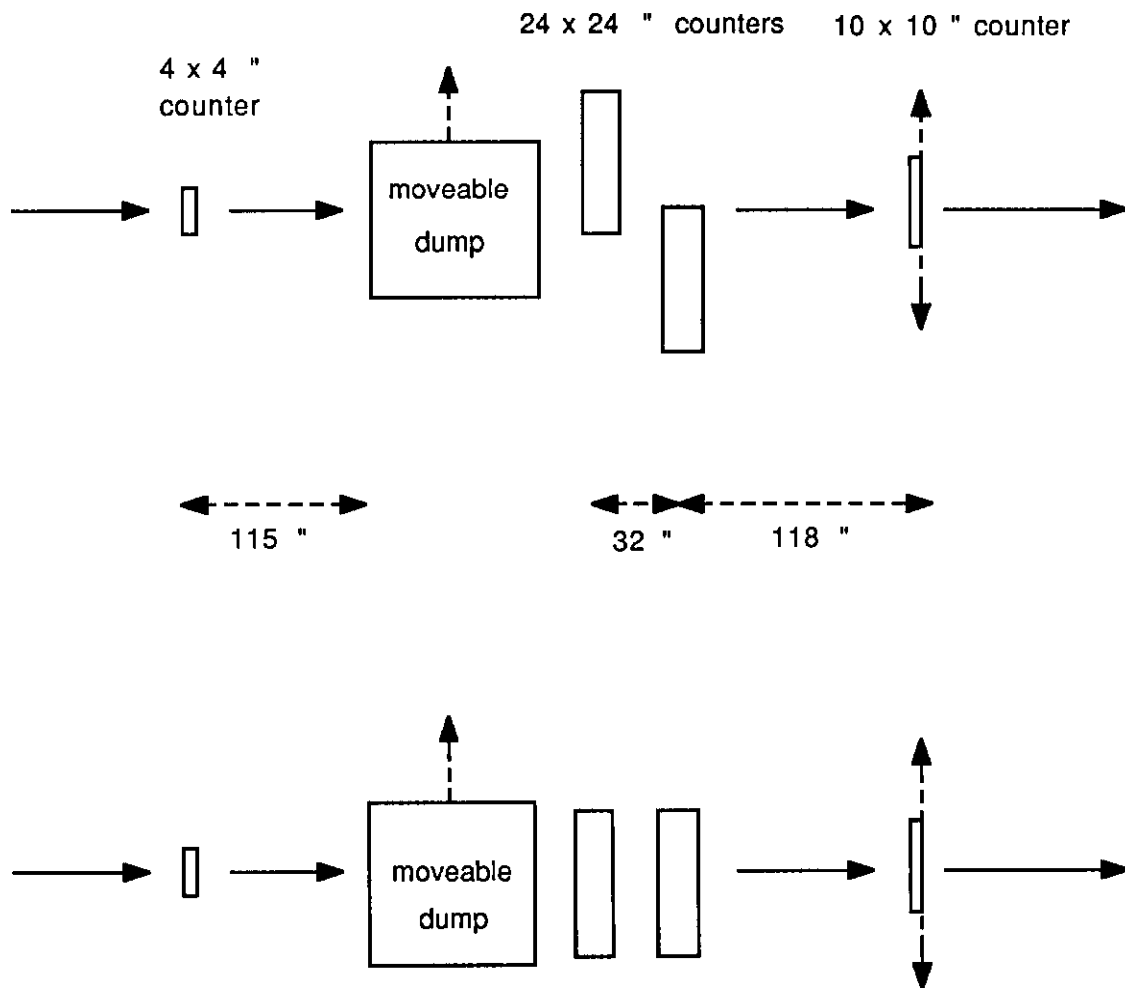


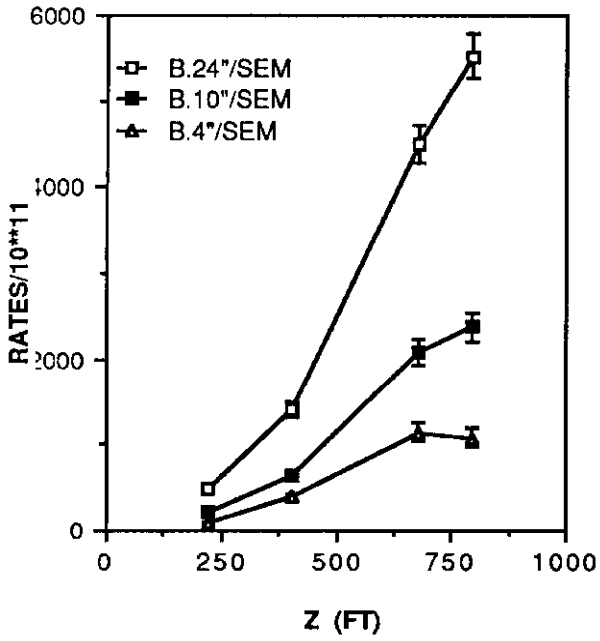
FIGURE 1



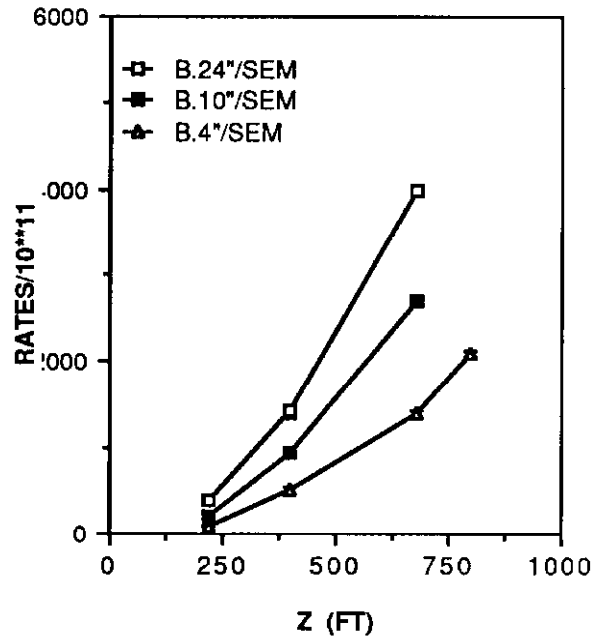
LAB F COUNTER LAYOUT

FIGURE 2

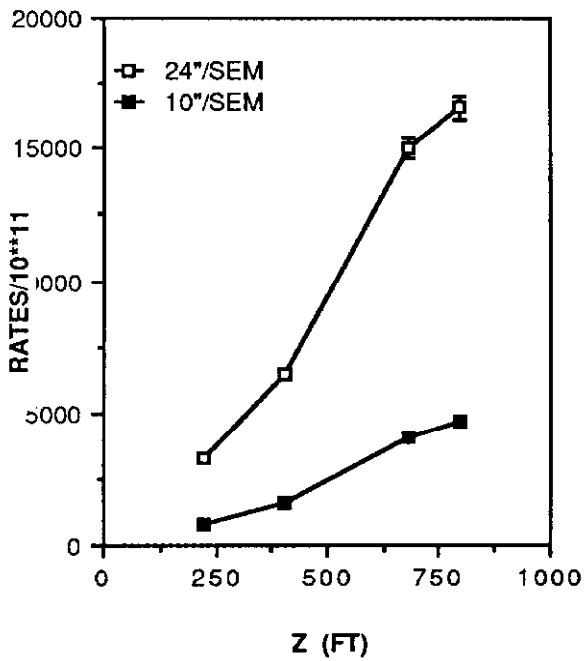
ZSCAN: HALO MONTE CARLO



ZSCAN: DATA



ZSCAN: HALO MONTE CARLO



ZSCAN: DATA

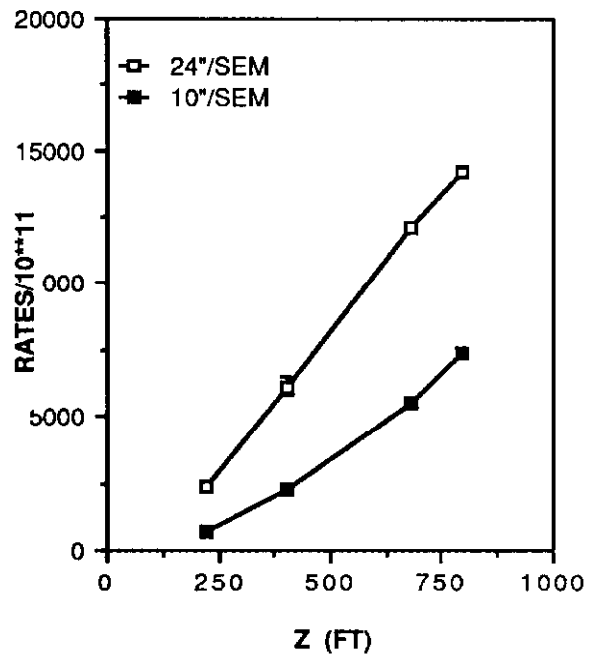


FIGURE 3

# HALO/BEAM RATIO FOR 200 GEV DATA

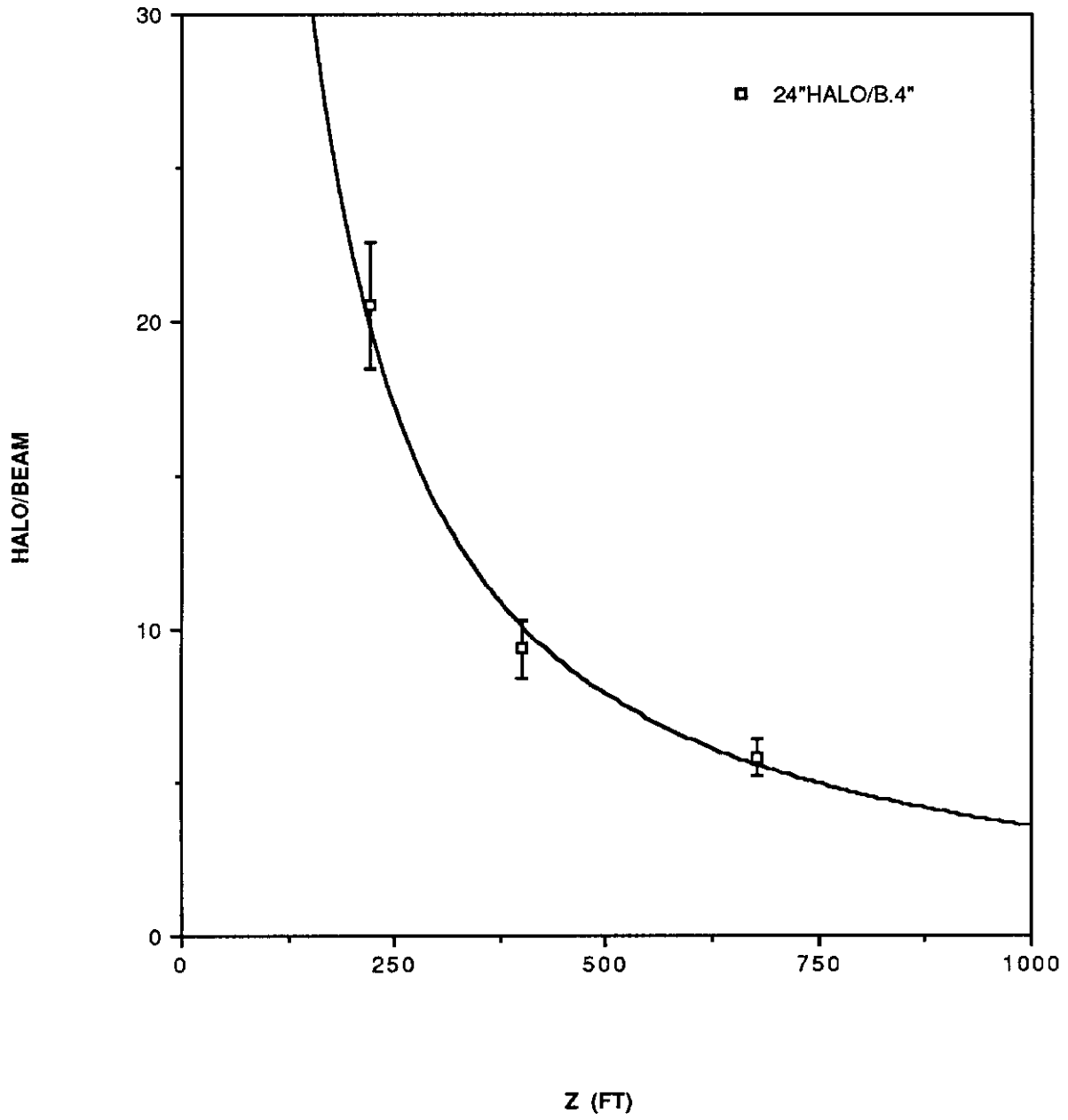
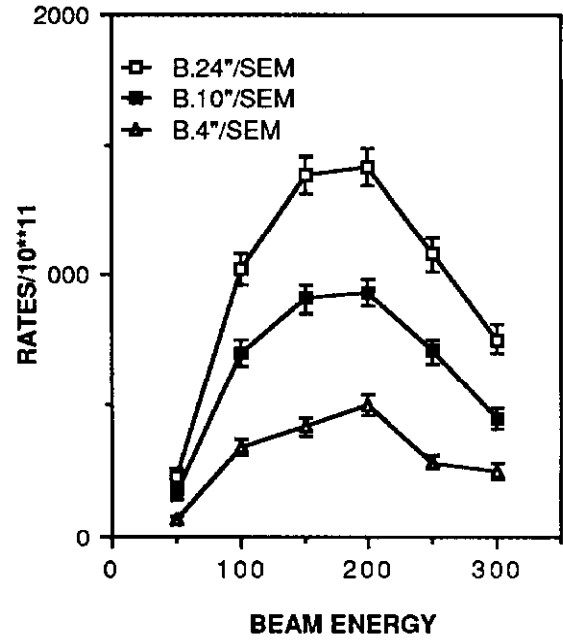
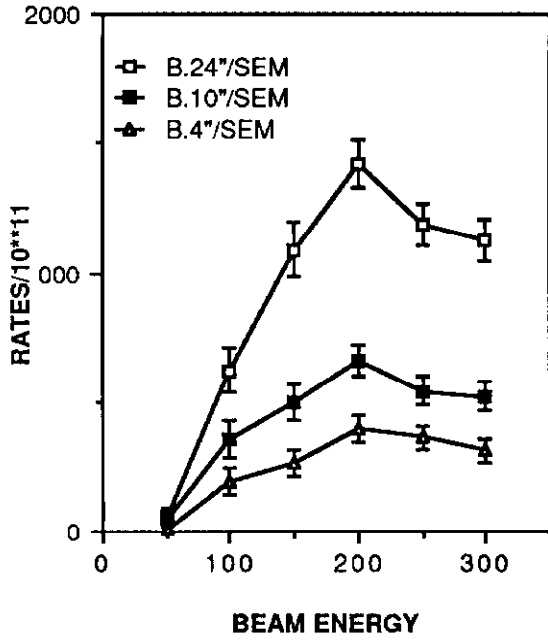


FIGURE 4

**ENERGY SCAN: HALO MONTE CARLO**

**ENERGY SCAN: DATA**



**ENERGY SCAN: HALO MONTE CARLO**

**ENERGY SCAN: DATA**

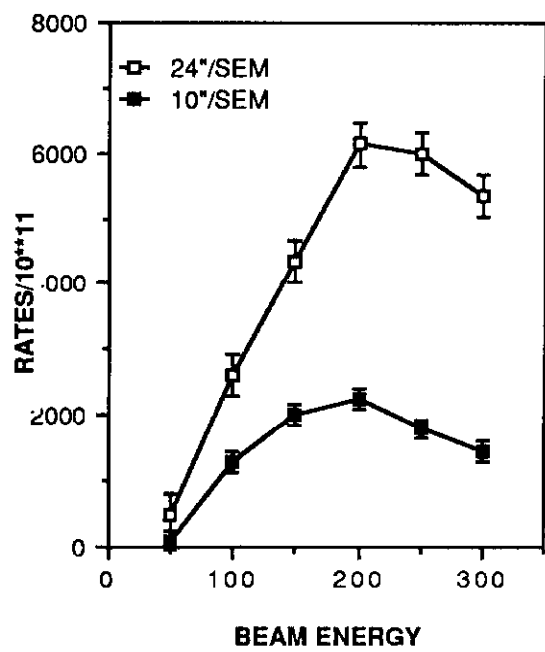
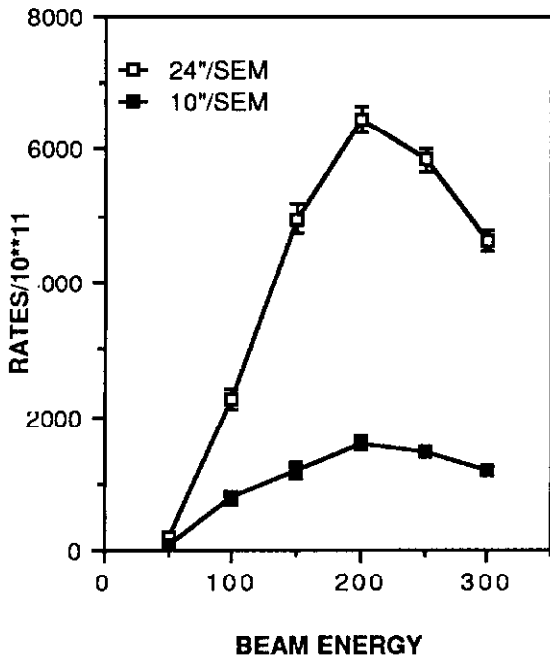


FIGURE 5

HALO/BEAM RATIO FOR BE/POLY IN NE9

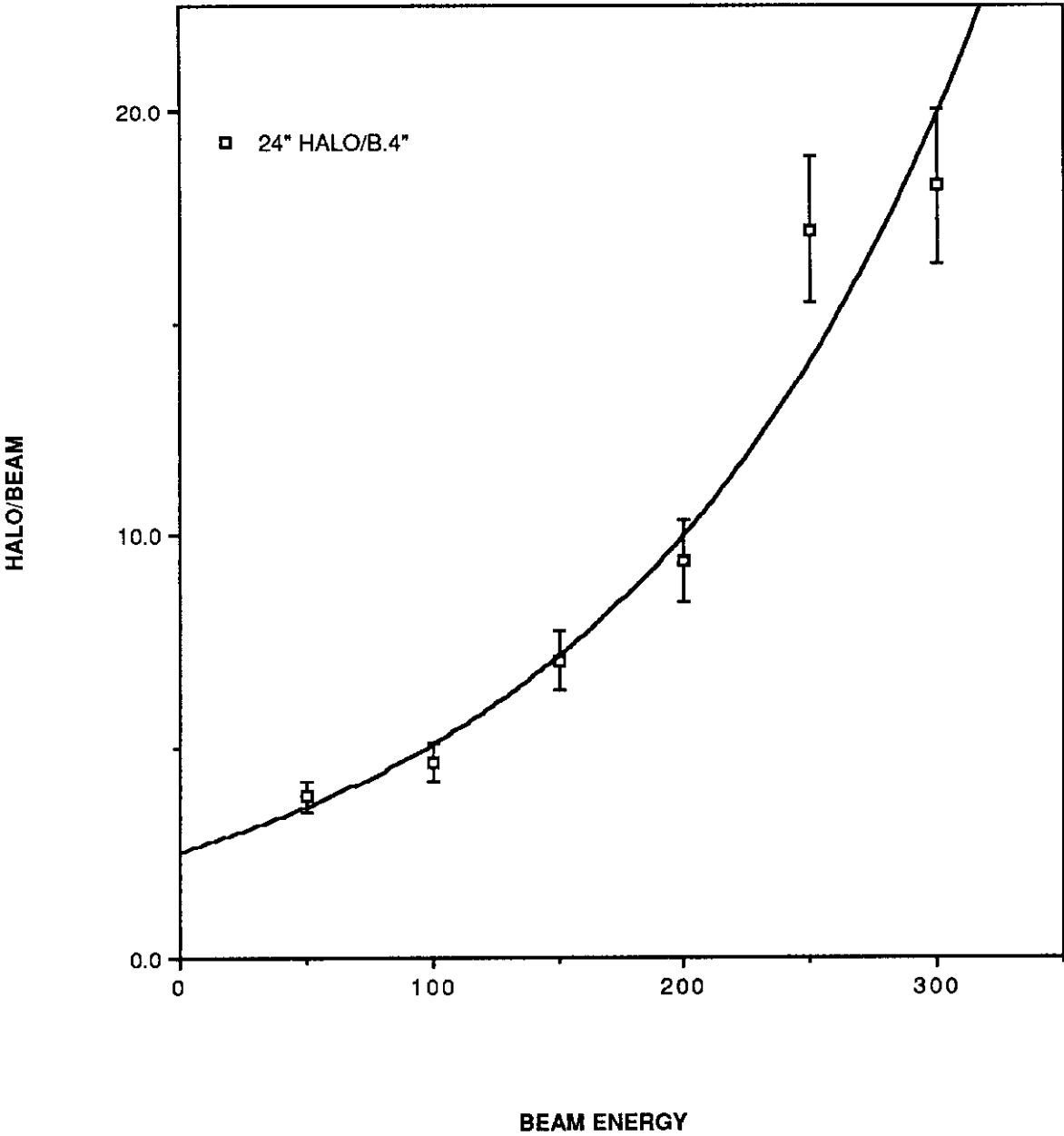
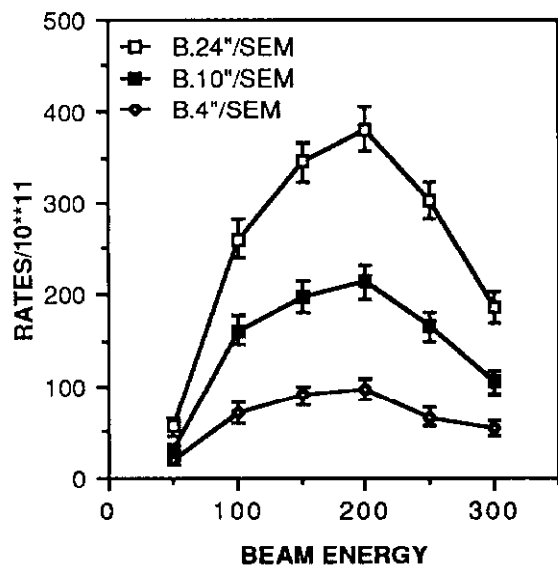
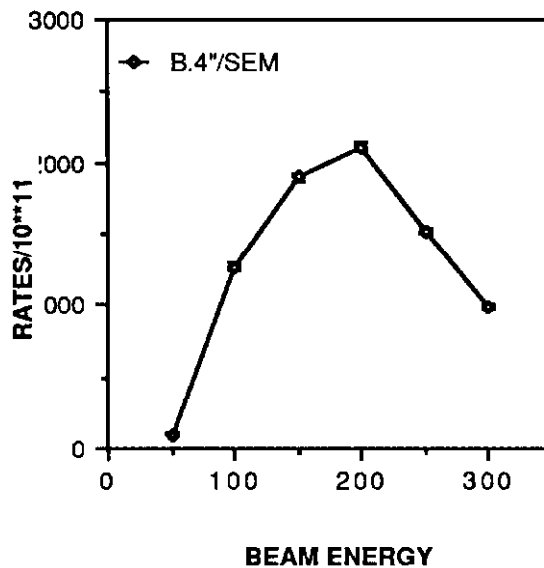


FIGURE 6

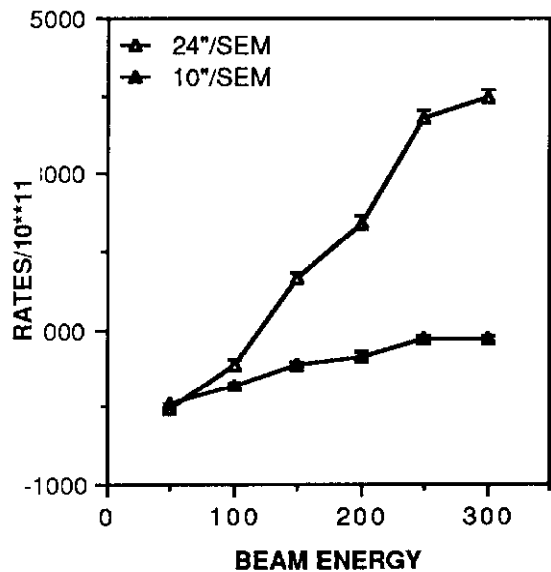
ENERGY SCAN: NT9CH=0



ENERGY SCAN: POLY IN NEB



ENERGY SCAN: NT9CH=0



ENERGY SCAN: POLY IN NEB

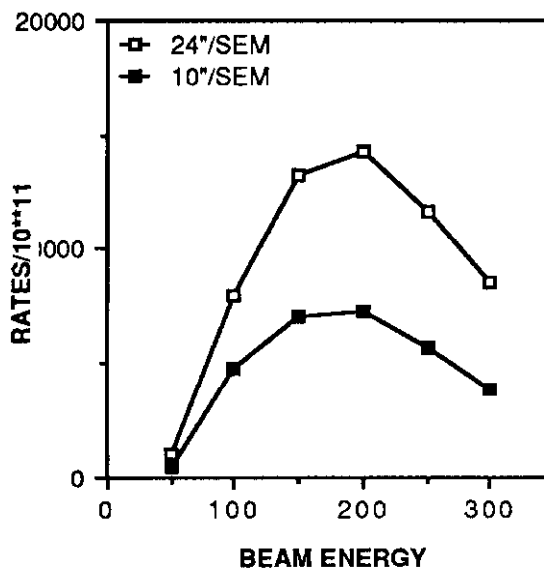
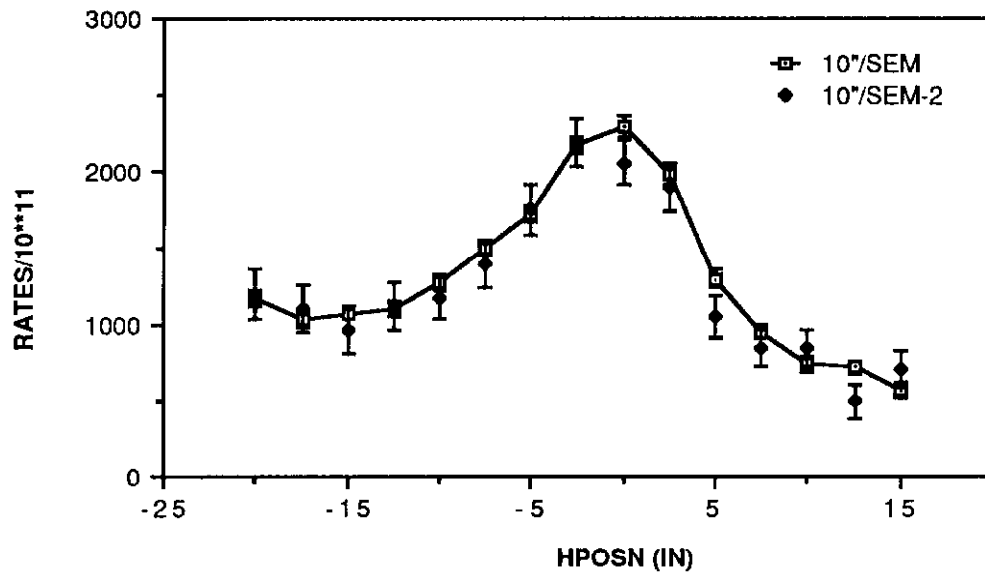


FIGURE 7

### 10" HORZ SCAN DATA SETS



### 10" VERT SCAN DATA SETS

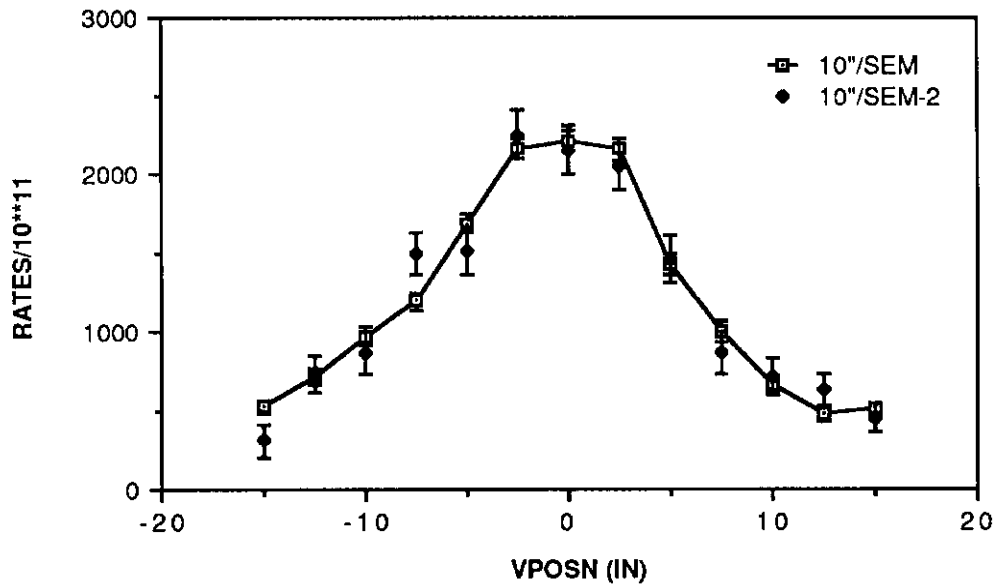
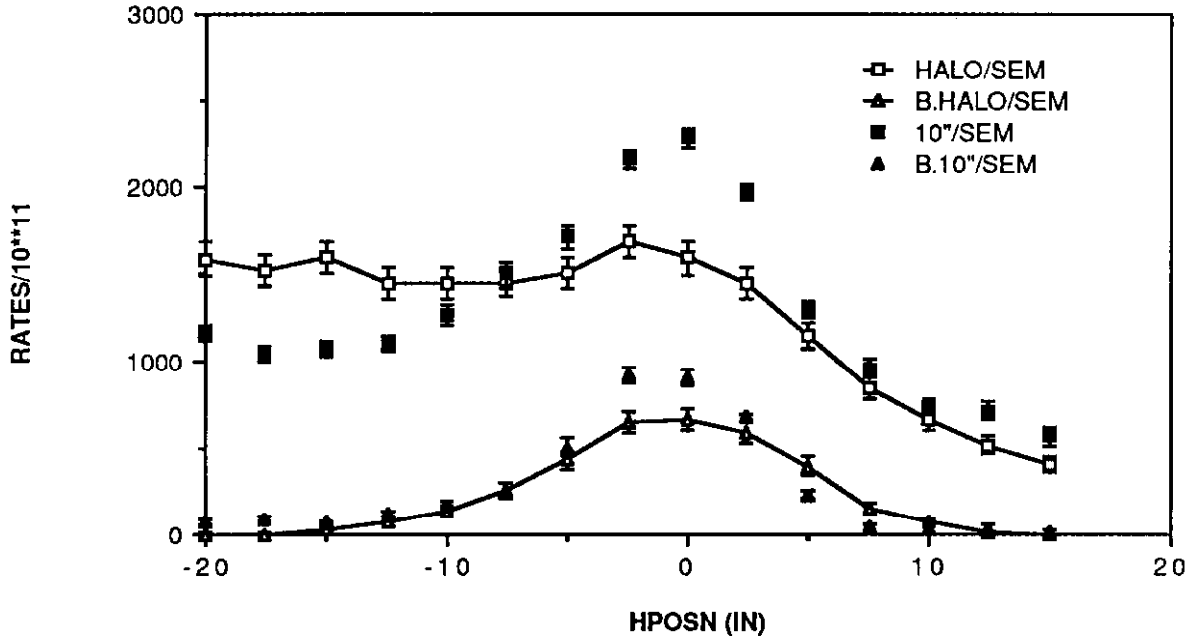


FIGURE 8

### HORIZONTAL SCAN AT 200 GEV



### VERTICAL SCAN AT 200 GEV

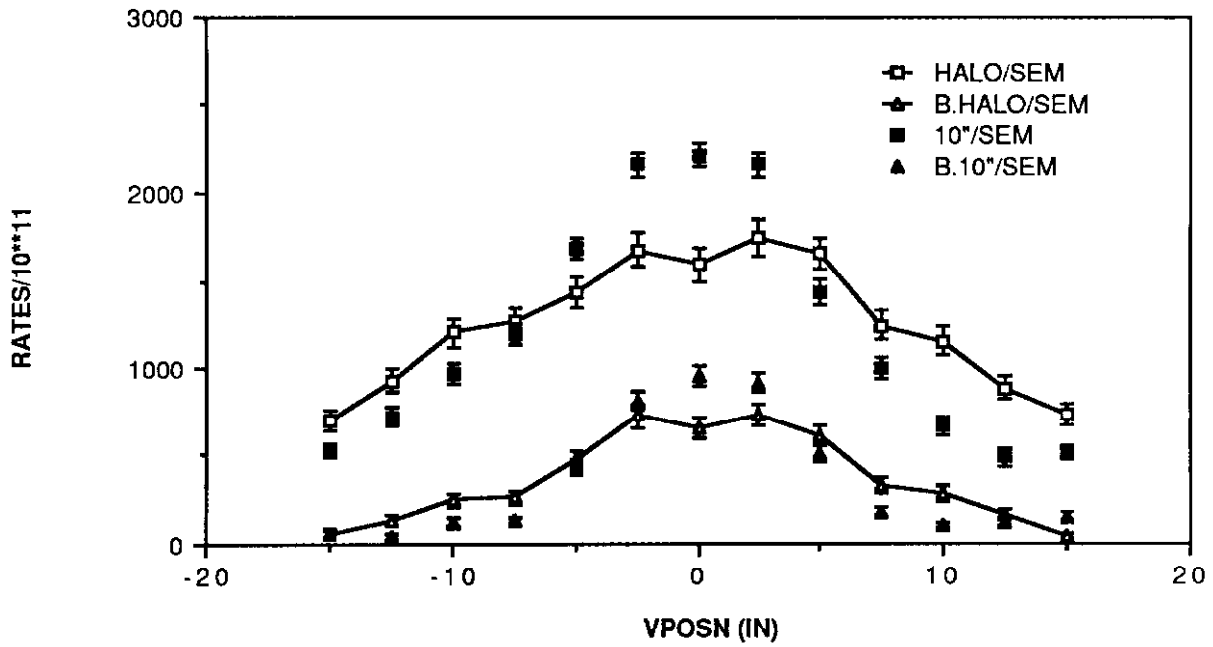
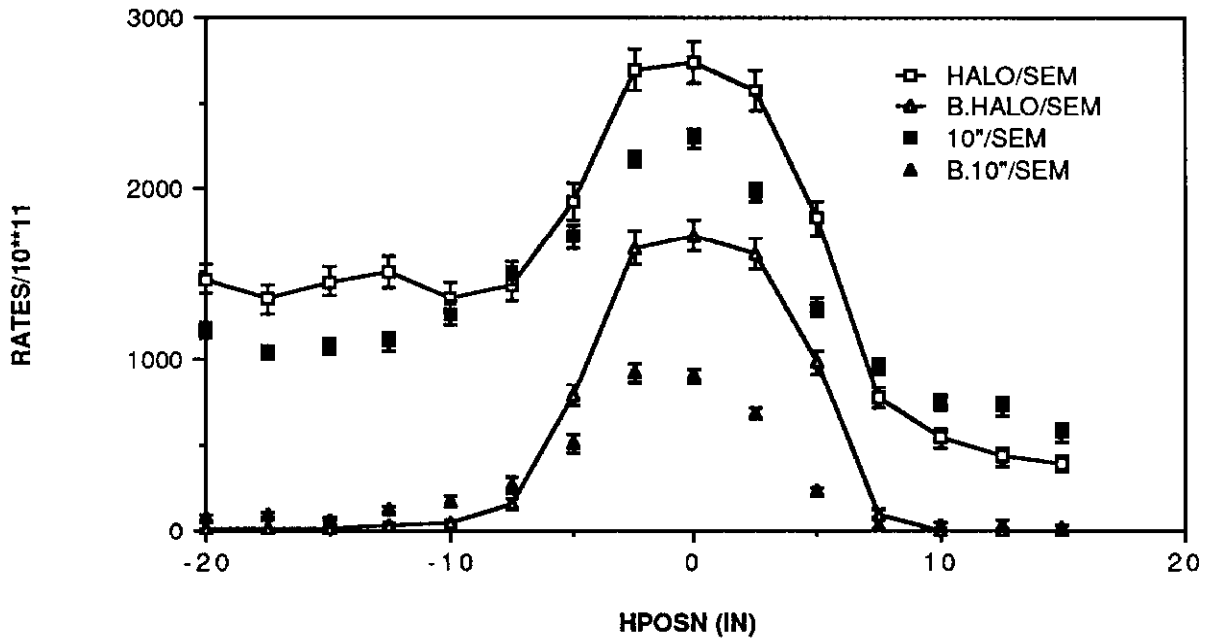


FIGURE 9

### HORIZONTAL SCAN AT 200 GEV - IDEAL -



### VERTICAL SCAN AT 200 GEV - IDEAL -

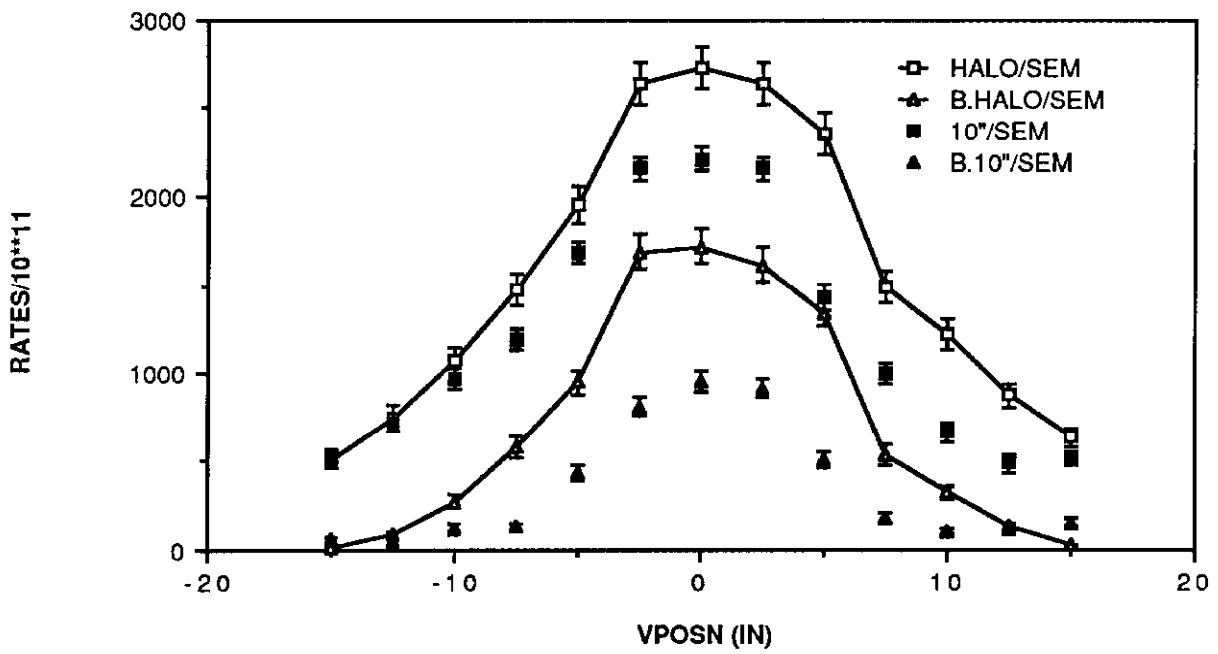
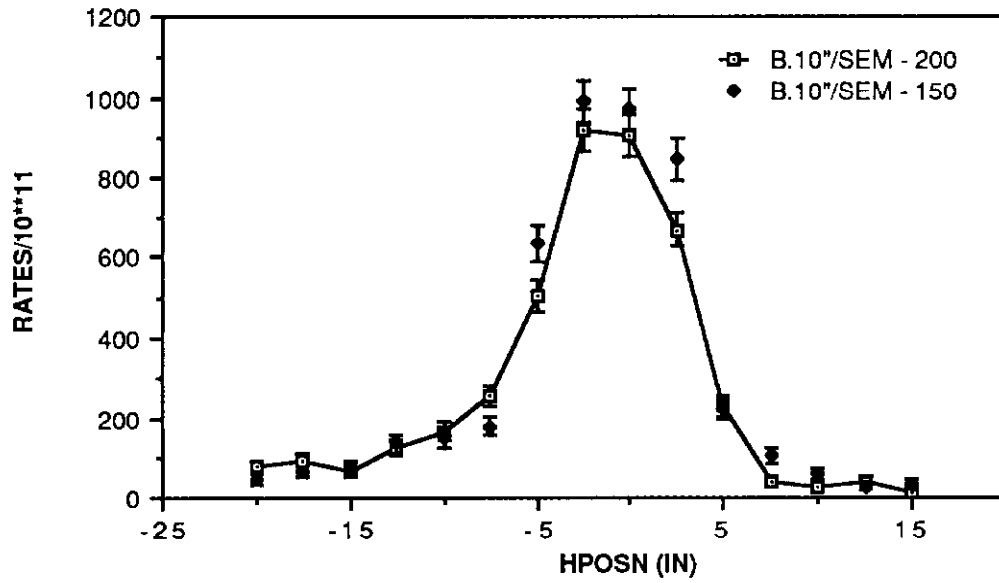


FIGURE 10

### 150 GEV VS 200 GEV HORZ DATA



### 150 GEV VS 200 GEV VERT DATA

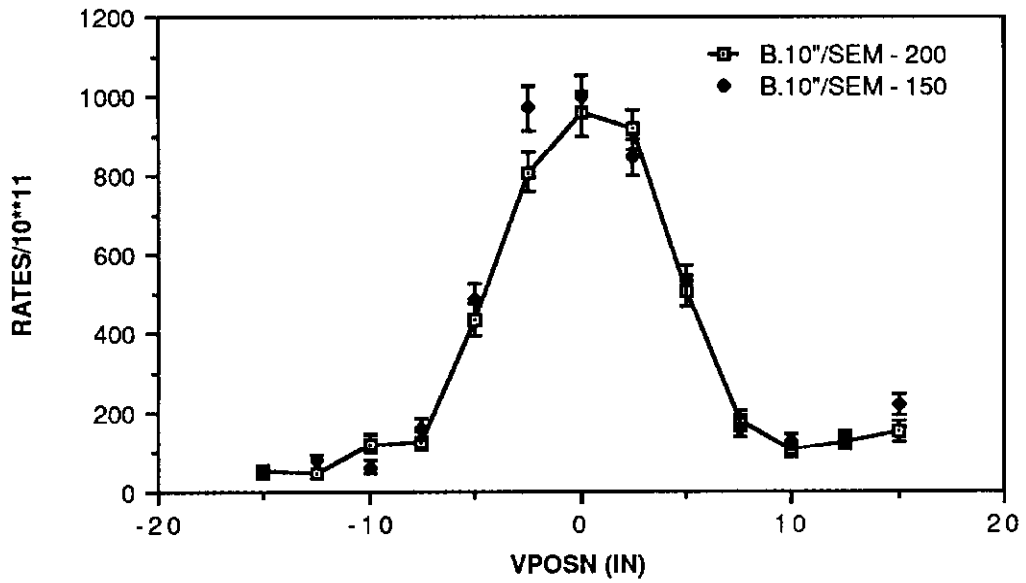
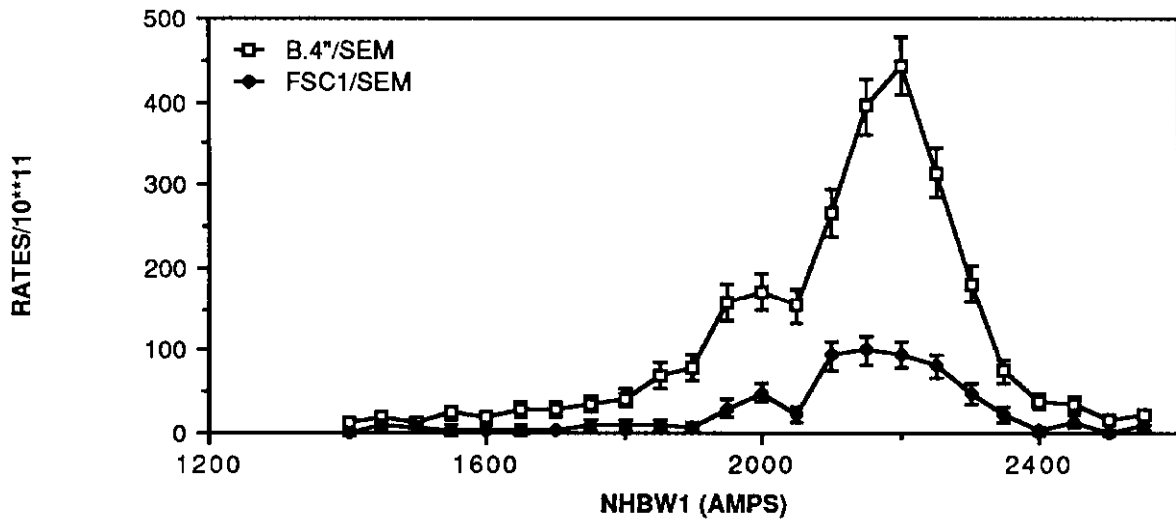
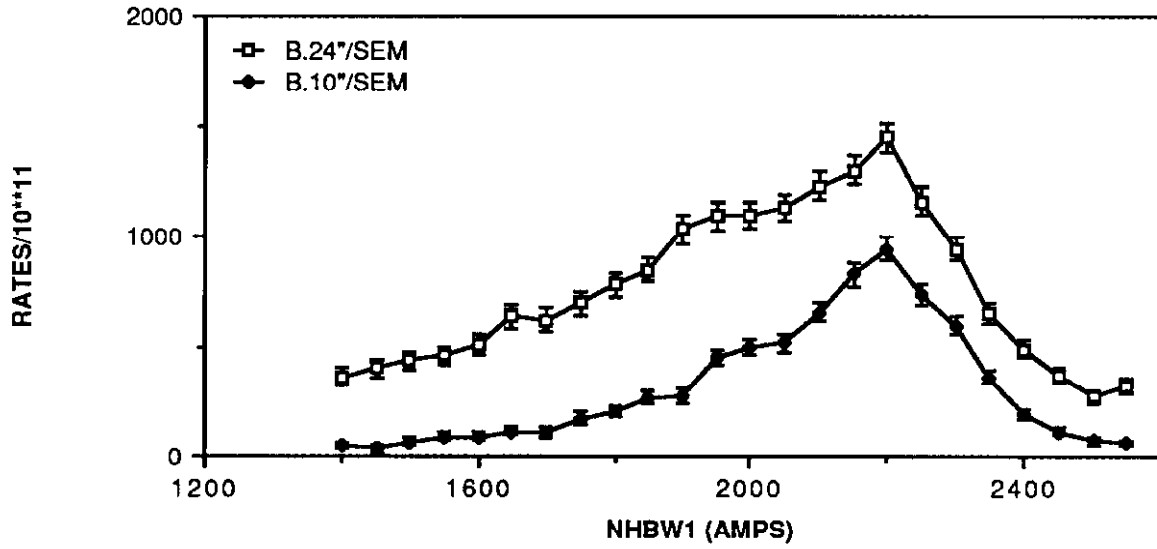


FIGURE 11

### MAGNET SCAN BE/POLY IN NE9



### MAGNET SCAN BE/POLY IN NE9



### MAGNET SCAN BE/POLY IN NE9

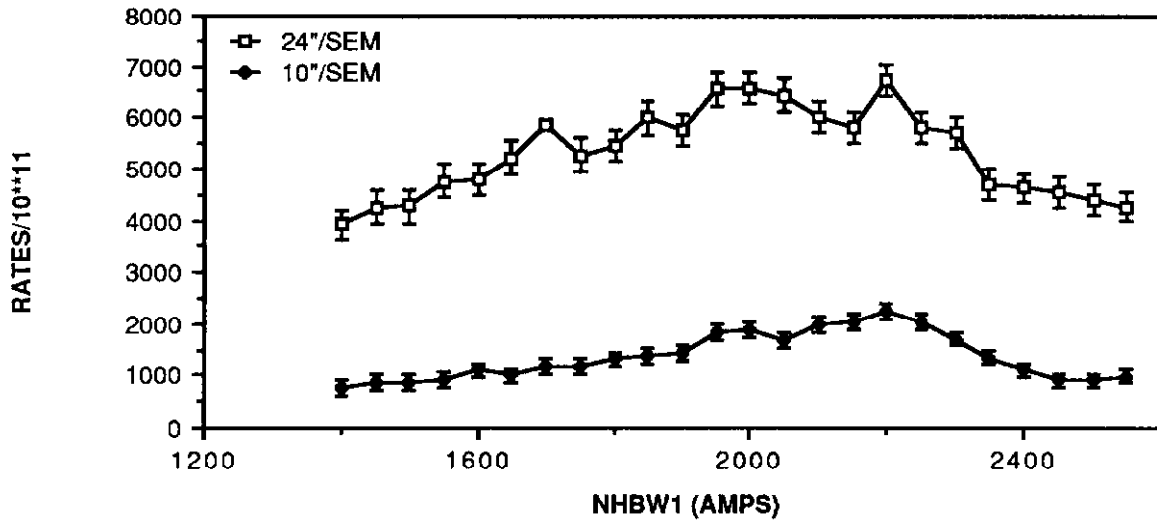
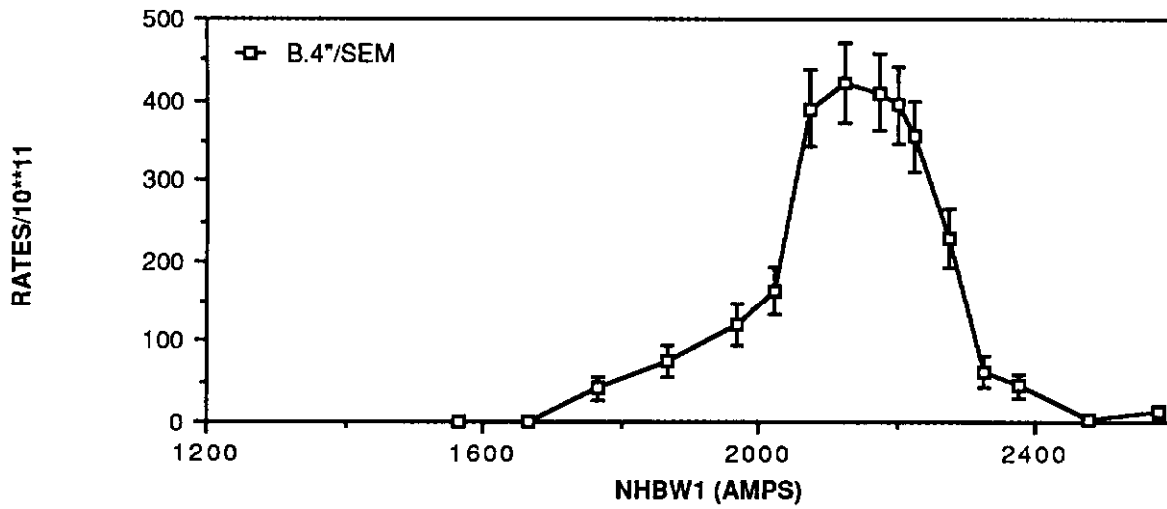
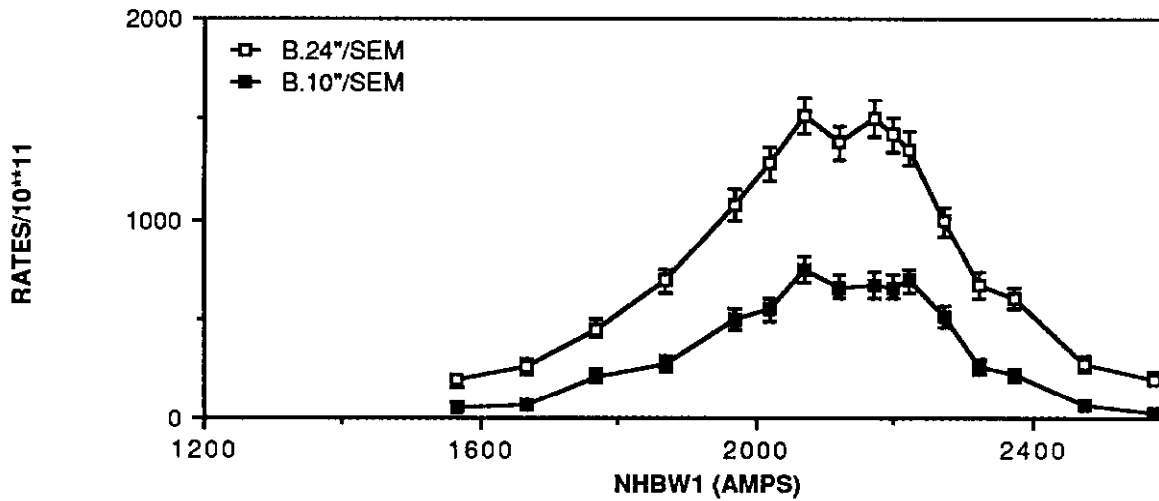


FIGURE 12

### MAGNET SCAN: HALO MONTE CARLO



### MAGNET SCAN: HALO MONTE CARLO



### MAGNET SCAN: HALO MONTE CARLO

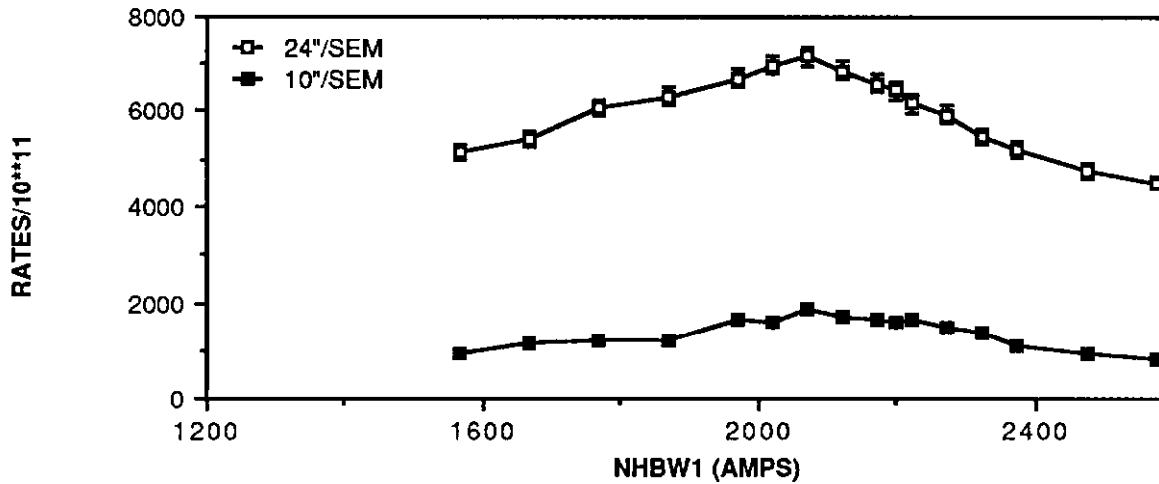
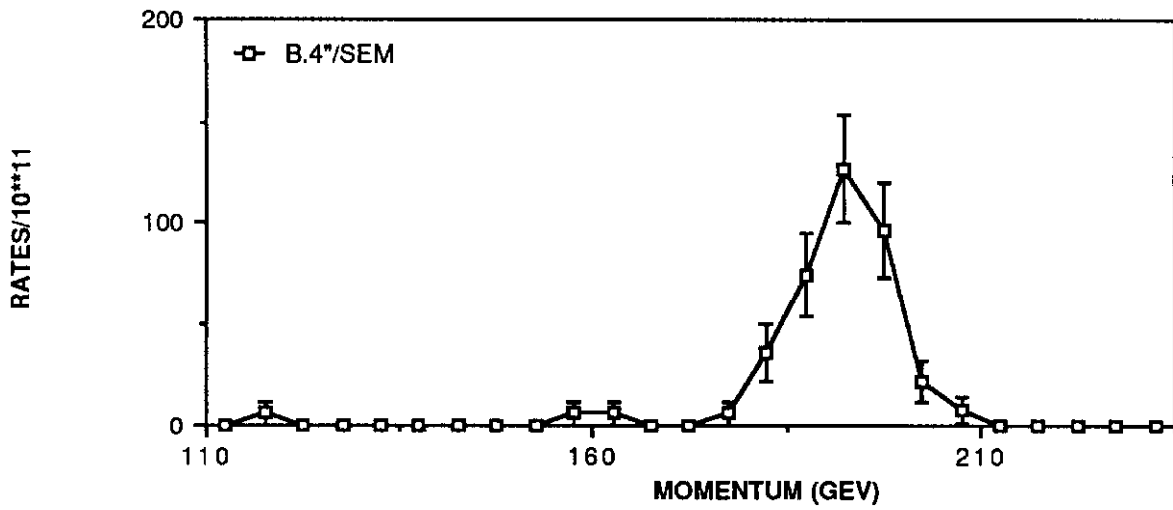
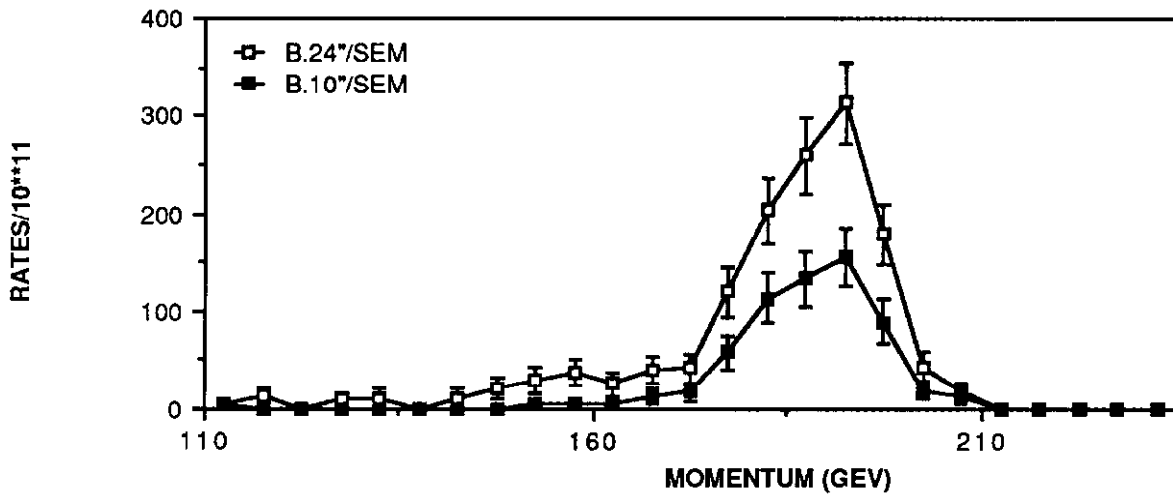


FIGURE 13

### MOMENTUM SPECTRA: HALO MONTE CARLO



### MOMENTUM SPECTRA: HALO MONTE CARLO



### MOMENTUM SPECTRA: HALO MONTE CARLO

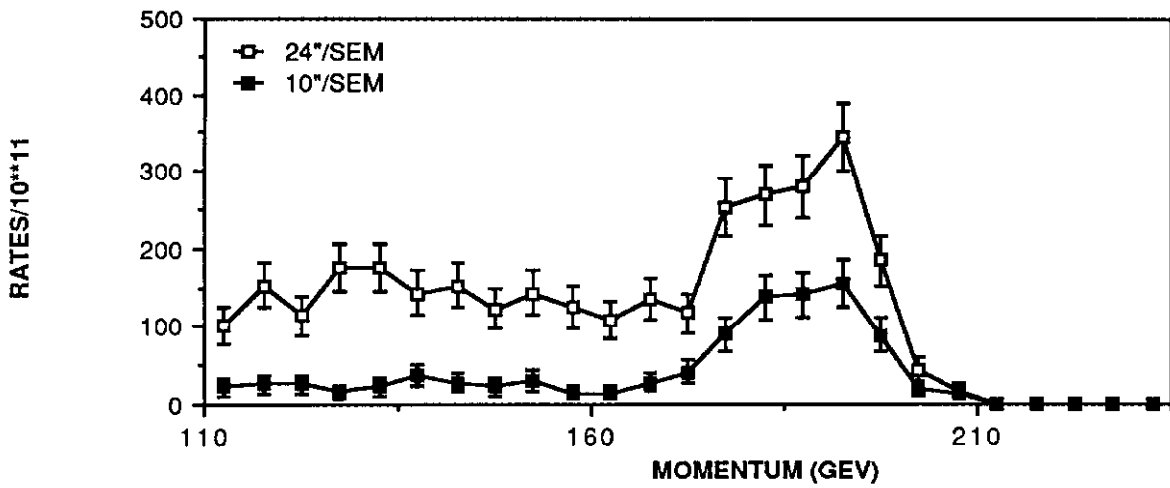
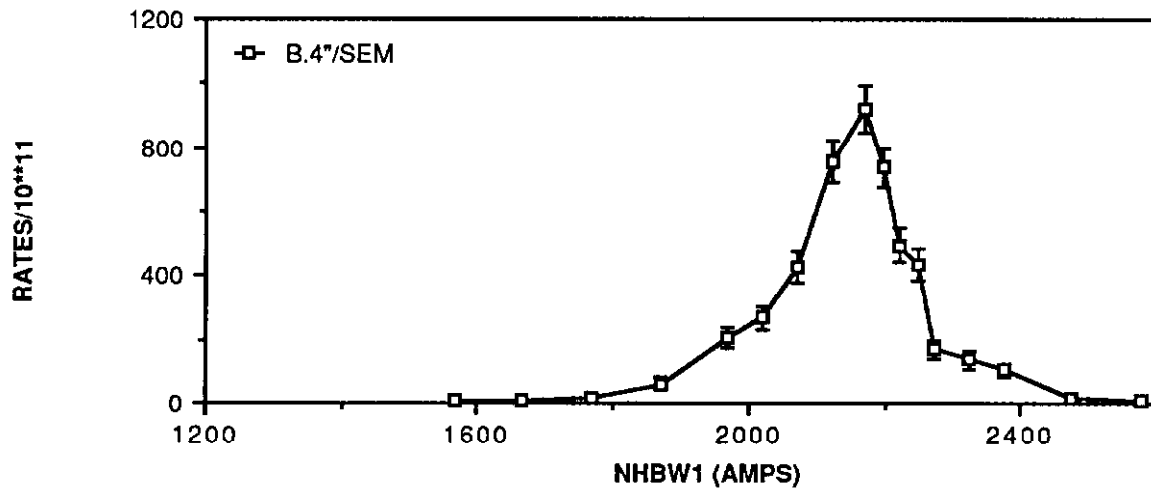
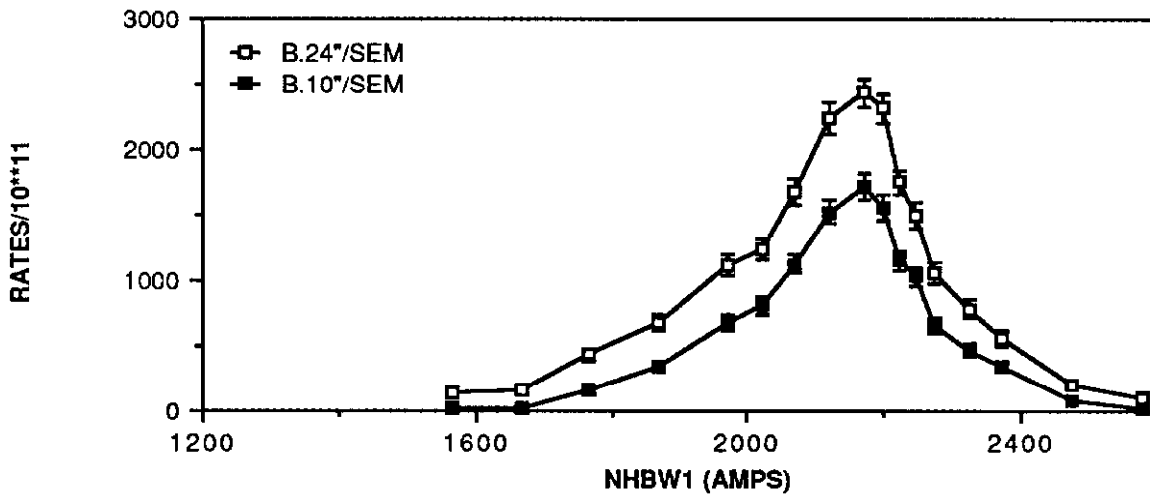


FIGURE 14

### MAGNET SCAN: HALO -IDEAL-



### MAGNET SCAN: HALO -IDEAL-



### MAGNET SCAN: HALO -IDEAL-

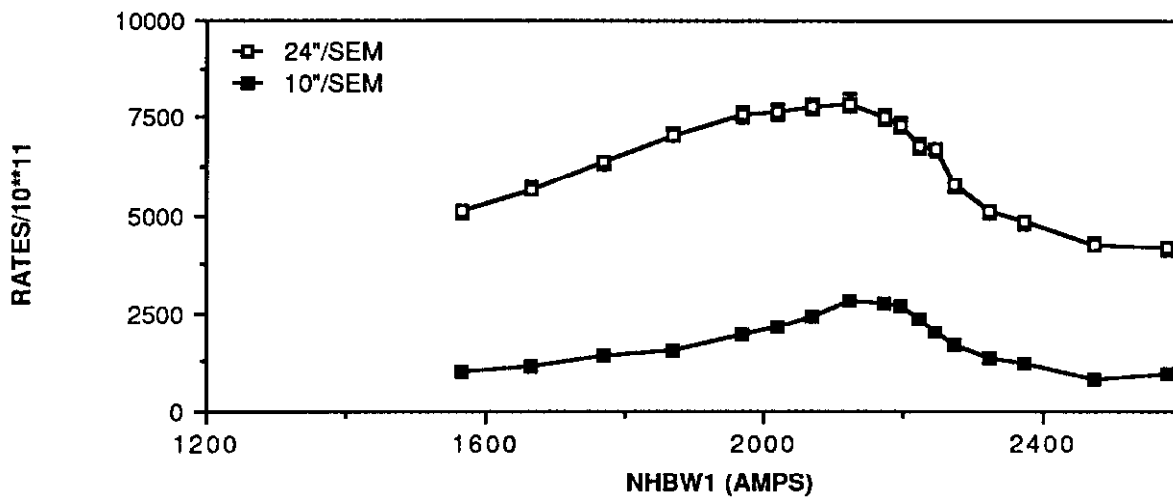
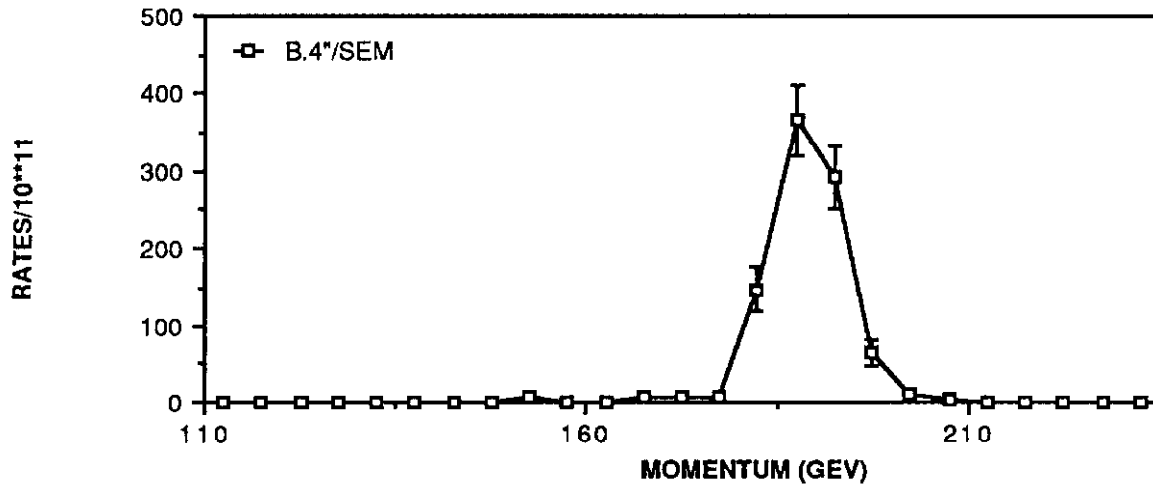
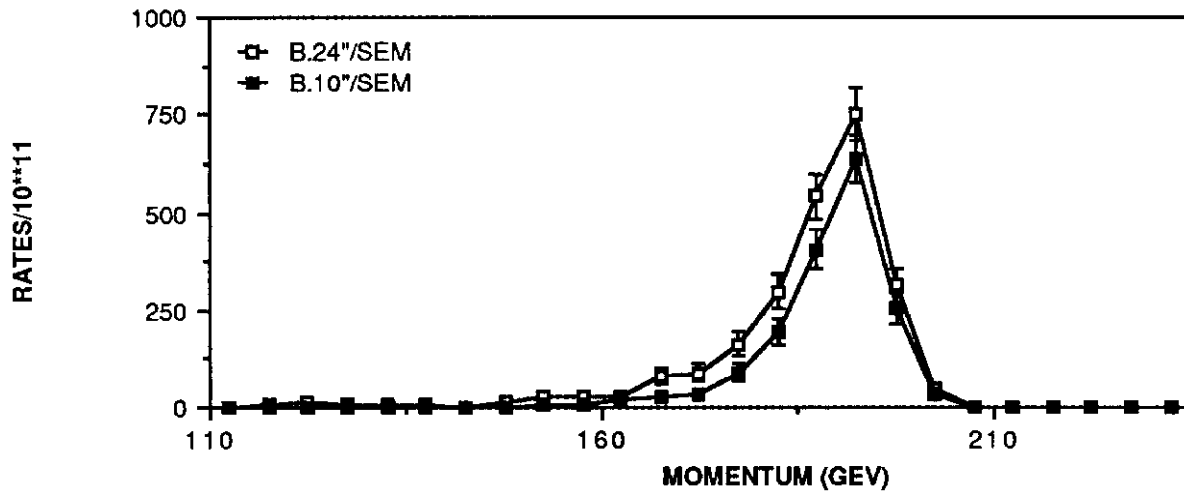


FIGURE 15

### MOMENTUM SPECTRA: HALO - IDEAL -



### MOMENTUM SPECTRA: HALO - IDEAL -



### MOMENTUM SPECTRA: HALO - IDEAL -

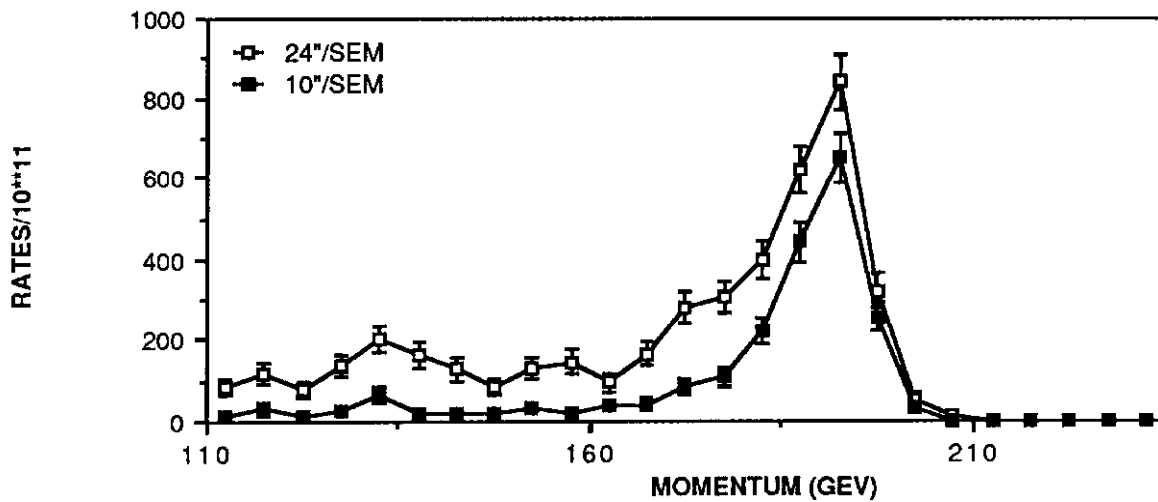


FIGURE 16